RSC Advances

PAPER

View Article Online
View Journal | View Issue

Cite this: *RSC Adv.*, 2021, **11**, 4921

Electrodynamic assisted self-assembled fibrous hydrogel microcapsules: a novel 3D *in vitro* platform for assessment of nanoparticle toxicity†

Shanta R. Bhattarai, ‡*[ab] Sheikh Saudi, ‡[c] Shalil Khanal,[d] Shyam Aravamudhan,[c] Checo J. Rorie[a] and Narayan Bhattarai *[e]

Nanoparticle (NP) toxicity assessment is a critical step in assessing the health impacts of NP exposure to both consumers and occupational workers. *In vitro* assessment models comprising cells cultured in a two-dimensional tissue culture plate (2D-TCP) are an efficient and cost-effective choice for estimating the safety risks of NPs. However, *in vitro* culture of cells in 2D-TCPs distorts cell–integrin and cell–cell interactions and is not able to replicate an *in vivo* phenotype. Three-dimensional (3D) *in vitro* platforms provide a unique alternative to bridge the gap between traditional 2D *in vitro* and *in vivo* models. In this study, novel microcapsules of alginate hydrogel incorporated with natural polymeric nanofibers (chitin nanofibrils) and synthetic polymeric nanofibers poly(lactide-*co*-glycolide) are designed as a 3D *in vitro* platform. This study demonstrates for the first time that electrodynamic assisted self-assembled fibrous 3D hydrogel (3D-SAF hydrogel) microcapsules with a size in the range of 300–500 μm in diameter with a Young's modulus of 12.7–42 kPa can be obtained by varying the amount of nanofibers in the hydrogel precursor solutions. The 3D-SAF microcapsules were found to mimic the *in vivo* cellular microenvironment for cells to grow, as evaluated using A549 cells. Higher cellular spreading and prolonged proliferation of A549 cells were observed in 3D-SAF microcapsules compared to control microcapsules without the nanofibers. The 3D-SAF microcapsule integrated well plate was used to assess the toxicity of model NPs, *e.g.*, Al_2O_3 and ZnO. The toxicity levels of the model NPs were found to be dependent on the chemistry of the NPs and their physical agglomeration in the test media. Our results demonstrate that 3D-SAF microcapsules with an *in vivo* mimicking microenvironment can be developed as a physiologically relevant platform for high-throughput toxicity screening of NPs or pharmaceutical drugs.

Received 28th October 2020
Accepted 7th January 2021

DOI: 10.1039/d0ra09189h

rsc.li/rsc-advances

Introduction

Emerging nanotechnology has brought about a great revolution in the industrial, agriculture, medicine, and public health sectors for the treatment of diseases, food safety, smart sensors and packing materials, *etc.*[1–3] The human population has been constantly exposed to a large variety of nanoparticles (NPs) *via* multiple sources such as consumable products, and air and water pollution, *etc.* For example, humans are readily exposed to titanium oxide (TiO_2) and zinc oxide (ZnO)[4,5] NPs in sunscreens and lotions, and silver (Ag)[6] NPs from band-aids and cosmetics.[7,8] Similarly, aluminum oxide (Al_2O_3) is a widely used material in prostheses, bionic implants, dental crowns, and other dental implants.[9,10] Although, the role of these NPs (*i.e.* TiO_2, ZnO, and Ag) in these products is to enhance the photo-optical or antibacterial properties or to provide inert coating (*i.e.* Al_2O_3), these nanomaterials are a health concern.[11] Because of their small size and enhanced surface interactions, NPs can easily enter into the human body and cross various biological barriers.[12] NPs can also eventually reach and stay for prolonged periods of time in the most sensitive organs of the human body.[13,14]

In vitro toxicity assessment of NPs[14–18] using two-dimensional tissue culture plates (2D-TCP) models is one of the highly efficient and cost-effective choices to remedy this issue,[18,19] and has been recommended by many regulatory authorities.[20–23] However, the culture of cells in 2D-TCP lacks the proper cell–cell and cell–matrix interactions and has not been able to replicate an *in vivo*

[a]*Department of Biology, North Carolina A&T State University, Greensboro, NC 27411, USA*

[b]*Department of Biological Science, Winston-Salem State University, Winston-Salem, NC 27110, USA. E-mail: bhattaraisr@wssu.edu*

[c]*Department of Nanoengineering, Joint School of Nanoscience and Nanoengineering, North Carolina A&T State University, Greensboro, NC 27411, USA*

[d]*Department of Applied Science and Technology, North Carolina A&T State University, Greensboro, NC 27411, USA*

[e]*Department of Chemical, Biological, and Bioengineering, North Carolina A & T State University, Greensboro, NC 27411, USA. E-mail: nbhattar@ncat.edu*

† Electronic supplementary information (ESI) available. See DOI: 10.1039/d0ra09189h

‡ Equal contribution.

phenotype.[24] In contrast to 2D-TCP, new 3D *in vitro* platforms provide a unique alternative to bridge the gap between traditional 2D *in vitro* and *in vivo* models, allowing for better replication of *in vivo* tissue function through 3D cell–cell and cell–matrix interactions and prolonged viability.[24–27] A variety of 3D cell culture approaches are currently being used, including cell-seeded hydrogels as well as scaffold-free cellular self-assembly strategies.[28,29]

Alginate hydrogel-based 3D spheroid *in vitro* platforms offer a broad range of biochemical and biophysical properties for cell morphogenesis and function.[30,31] However, they require additional chemical or physical modification to introduce adhesion sites for cells.[32,33] Furthermore, the morphology of alginate hydrogels often does not mimic the filamentous nature of tissue extracellular matrix (ECM), which controls the spatial organization of the cell-adhesive ligands and mechanical signal transduction from cells to the ECM.[33] Also, the chemical modification and functionalization of alginate hydrogels is cost- and labor-intensive, and they are not readily remodeled by cells.[34,35] Therefore, current research has been focused to develop 3D hydrogel scaffolds using polymers of both biocompatible and biodegradable origin, such as alginate,[27] chitin,[36] and poly(lactide-*co*-glycolide) (PLGA)[37] as a potential strategy towards the development of realistic *in vivo* 3D ECM matrix.

Self-assembled nanofibrous hydrogel microcapsules allow for spatiotemporal control over chemically crosslinked gels that do not recapitulate the nanofibrillar structure of the ECM. We hypothesized that PLGA nanofiber/chitin nanofibrils containing microcapsules will have closer proximity to natural ECM features. The first goal of this study was to construct the fibrous alginate hydrogel microcapsules that have random layers of both synthetic and natural nanofibers for the purpose of creating a better microenvironment for cell growth and proliferation. Our research group has been focused on establishing electrostatic encapsulation, also called electrodynamic technology, to generate fibrous hydrogel microcapsules as 3D cell culture platforms.[27] This is the first report on the fabrication of fibrous hydrogel microcapsules containing self-assembled synthetic and natural nanofibers that are crosslinked, either chemically or physically, to form a 3D network. The second goal of this study was to evaluate the feasibility of utilizing hydrogel microcapsules with cells as a platform for the screening of NP toxicity. This study is the essential first step for our future work aimed on developing a cost-effective nano-toxicity screening device that marries an integrated well plate and fibrous hydrogel microcapsule system.

We synthesized various compositions of self-assembled fibrous 3D hydrogel (3D-SAF hydrogel) microcapsules of alginate with nanofibers/nanofibrils of PLGA and chitin. Prior to evaluating the cell encapsulation ability of 3D-SAF microcapsules with A549 cells, the impact of nanofibers on the morphology and mechanical properties of the microcapsules were thoroughly evaluated. The cell encapsulated 3D-SAF microcapsules were then used as an *in vitro* 3D cell culture model to assess the toxicity of the NPs. This is a proof-of-concept study on how nanofibrous microcapsules can provide new insight on 3D *in vitro* microenvironments that influence the progression of 3D models for high throughput nano-toxicity screening applications.

Results

Fabrication and characterization of the 3D-SAF hydrogel microcapsules

Fig. 1 shows a schematic diagram of the overall design of the 3D-SAF microcapsules including the capability to engineer materials and devices using three biopolymers, suitable for the high throughput toxicity screening of NPs in a microcapsule-based miniaturized 3D cell culture. The interpenetrating nano-network structure of chitin nanofibrils and PLGA nanofibers in alginate microcapsules provides an ECM mimicking microenvironment for the encapsulated cells that eventually mimics cells *in vivo*.

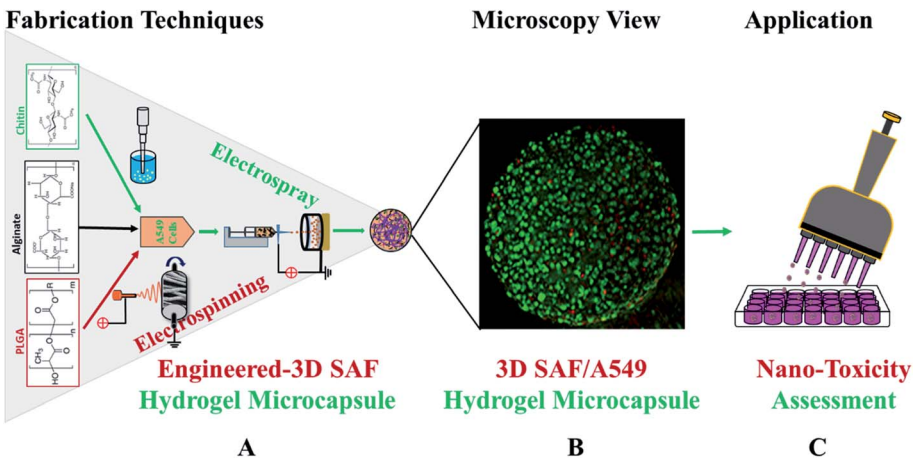

Fig. 1 Schematic diagram showing the overall design and production of electrodynamic assisted 3D-SAF hydrogel microcapsules for toxicity testing. (A) Synthesis scheme of the 3D-SAF microcapsules, (B) fluorescent dye-labeled A549 cell encapsulated 3D-SAF microcapsules, and (C) expected capability of the high throughput nanotoxicity screening device. Electrospun nanofibers of PLGA were first converted into cryoground fiber powder and then dispersed in alginate solution along with chitin nanofibrils. Hydrogel precursor solution was mixed with cell suspension and then applied for electrostatic encapsulation to prepare cell microcapsules. Cells in the microcapsule were stained with acridine orange and propidium iodide (AOPI) dye, where green and red colors indicate live and dead cells, respectively.

Fibrous microcapsules comprising cryoground nanofibers of PLGA, chitin nanofibrils, and alginate hydrogel were obtained using an electrospray assisted and divalent cation triggered self-assembly technique. Electrospray parameters including voltage, distance to the collector, solution viscosity, and flow rate were optimized similarly to in our previous publication.[27] Composition dependent surface morphology and size of the microcapsules were observed as shown in Fig. 2.

The diameter of the fully swollen microcapsules measured in the cell culture media was in the range of 300 to 500 μm. The average diameters of the as-prepared microcapsules were 361.38 ± 17 μm, 328.11 ± 14 μm, 353.26 ± 14 μm, 344.17 ± 19 μm, 320.87 ± 9 μm, and 470.91 ± 13 μm for SAF-0, SAF-10, SAF-20, SAF-30, SAF-50, and SAF-100, respectively. Among all the compositions, PLGA nanofibers containing 3D SAF hydrogel microcapsules were relatively smaller in size, and several black patchy structures were observed under an optical microscope. Upon the addition of chitin nanofibrils into the alginate gel precursor, the distribution of PLGA nanofibers in the microcapsules was improved significantly. The dark black spots of SAF-10 indicated that PLGA nanofibers alone produced non-homogenously distributed fibrous microcapsules (ESI S1†). We previously demonstrated[27] that using a higher amount of PLGA nanofibers yields denser fiber-networks in the hydrogel that produce nonhomogeneous microcapsules with more compact aggregates of fibers surrounded by a permeable hydrogel layer. Upon the addition of a different amount of chitin nanofibrils, the microcapsules turned more compact and opaque. Under microscopy observation, no out-diffused nanofibers were observed from the microcapsules in the media. This observation further proved that there was no loss of nanofibers/nanofibrils during the electrospray process and that almost all of the nanofibers/nanofibrils were gelled with alginate during the microcapsule fabrication. More interestingly, the greatest benefit of the chitin nanofibrils was found to be in maintaining the aqueous stability, size and structure uniformity, and promoting greater physio mechanical integrity of the SAF microcapsules even upon changing the culture medium during the aqueous stability assessments, for up to several weeks. These are encouraging steps towards the application of SAF microcapsules in cell encapsulation study.

Mechanical properties of the 3D SAF hydrogel microcapsules

The mechanical properties of the 3D SAF microcapsules were studied by analyzing the force–displacement curve, obtained from compression tests on a single microcapsule ($n = 3$ for each composite). A schematic representation of the compression tests is shown in Fig. 3A, in which a fully swollen microcapsule in cell culture media was used to sandwich two parallel plates by moving the top plate while the bottom plate was kept stationary. The deformation of the tested samples was fixed up to 30% of their original diameter. The force–displacement curve obtained from the compression tests showed a hysteresis loop under compression and release of the force. A smooth hysteresis loop (Fig. 3B) was observed for pure alginate microcapsules (SAF-0), whereas the microcapsules with different nanofibers/nanofibril compositions exhibited a non-uniform deformation loop. One of the representative samples that shows non-uniform deformation under compression is shown in S2 in the ESI.† Such non-uniformity was most likely due to the uneven distribution of compressive force in the presence of nanofibers/nanofibrils

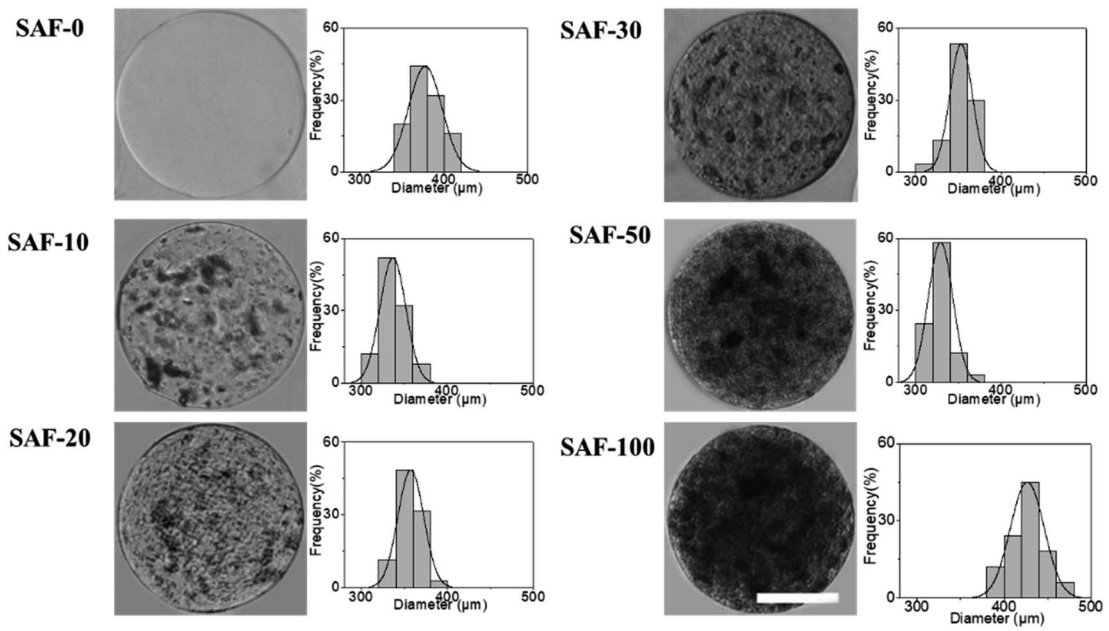

Fig. 2 Characterization of the 3D-SAF hydrogel microcapsules. Optical images of representative SAF hydrogel microcapsules and their respective size distribution were thoroughly evaluated. Microcapsules without fibers were soft and transparent (as shown in the SAF-0 composition), whereas microcapsules with fibers were opaque and hard (as shown in the SAF-10 to SAF-100 compositions). Scale bar = 200 μm.

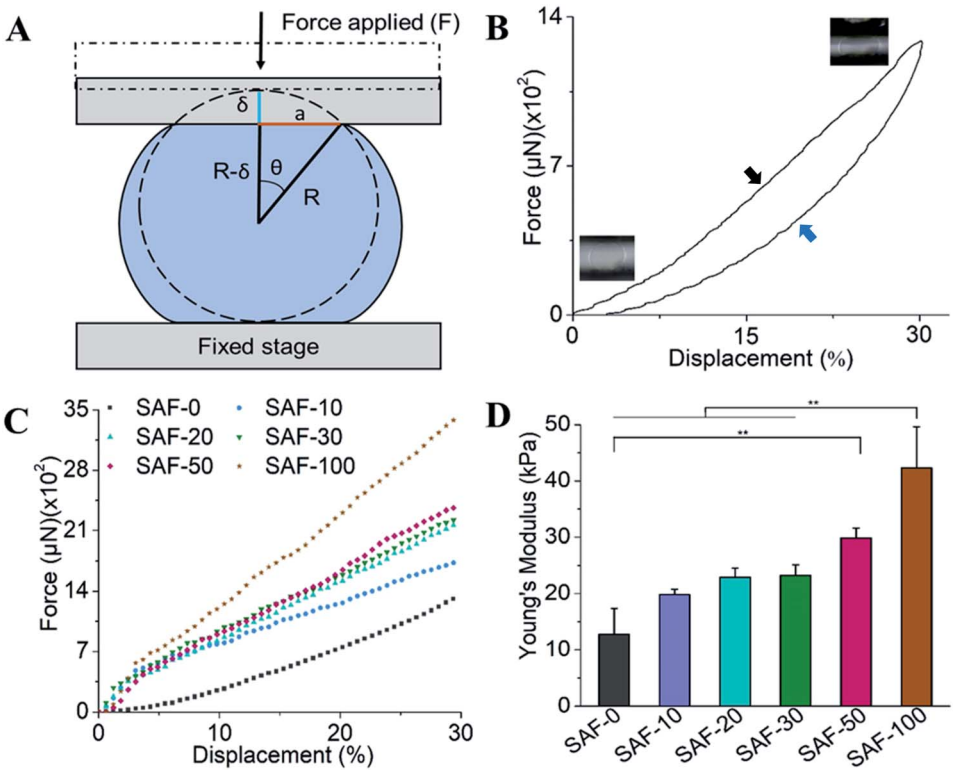

Fig. 3 Mechanical properties of the 3D SAF hydrogel microcapsules. (A) Schematic representations of the compression tests of the microcapsules between two parallel plates, (B) hysteresis loop of force *vs.* the displacement of a single microcapsule. The upper portion of the graph (black arrow) is due to compression force and the lower portion (blue arrow) represents the release force, (C) force (μN) *vs.* displacement (%) graphs, (D) Young's modulus of microcapsules with different compositions. Compressive properties of the materials were investigated by subjecting them to a maximum 30% strain corresponding to the original diameter of the microcapsules for 20 seconds.

in the sphere. For a comparison study of the SAF microcapsules, we compared the force–displacement curves under compression only (Fig. 3C). The force–displacement curves of the different compositions indicated that more force was needed for the same displacement as the concentration of the nanofibers/nanofibrils increased in the microcapsules.

The Young's modulus (E) of the microcapsules was calculated using the following equations provided by the equipment manufacturing company:

$$E = \frac{3(1-\nu^2)F}{4\delta a} - \frac{f(a)F}{\pi\delta} \quad (1)$$

$$f(a) = \frac{2(1+\nu^2)R^2}{\left(a^2+4R^2\right)^{3/2}} + \frac{(1-\nu^2)}{\left(a^2+4R^2\right)^{1/2}} \quad (2)$$

$$\theta = \cos^{-}\left[\frac{R-\delta}{R}\right] \quad (3)$$

$$a = (R-\delta)\tan\theta \quad (4)$$

where 'R' is the spherical radius of a microcapsule, 'δ' is the displacement, 'a' is the radius of contact area, 'ν' is the Poisson's ratio (0.5), 'F' is the applied force and 'E' is the Young's modulus.

The average modulus of the 3D SAF microcapsules ($n = 3$ for each composition) increased significantly from SAF-0 to SAF-100, ranging from 12.7 ± 4.6 to 42.3 ± 7.3 kPa, respectively (Fig. 3D), indicates that the mechanical stiffness increased upon increasing the amount of chitin nanofibrils in the microcapsules.

Cell encapsulation study of the 3D SAF hydrogel microcapsules

After analyzing the morphology and mechanical properties of the SAF microcapsules, a cell encapsulation and viability study was performed using the human epithelial cell line, A549. As shown in Fig. 4A, all of the microcapsules were spherical in shape with densely populated cell aggregates. Highly stable and good permeable SAF microcapsules were obtained by adding a higher amount of chitin nanofibrils. Upon changing the culture medium during the experiments, no phase separation of chitin and PLGA with alginate was observed in the SAF microcapsules. The size and stability of the SAF microcapsules were not changed in both under the preparation conditions and during storage in cell culture medium with the serum supplements. Some out-diffusion of cells from the microcapsules was observed in the SAF-0 and SAF-10 hydrogel microcapsules after 10 days of culture (ESI S3†). However, no empty microcapsules were observed microscopically. For all other compositions, there was no out-diffusion of cells from the SAF microcapsules and the cells were almost uniformly

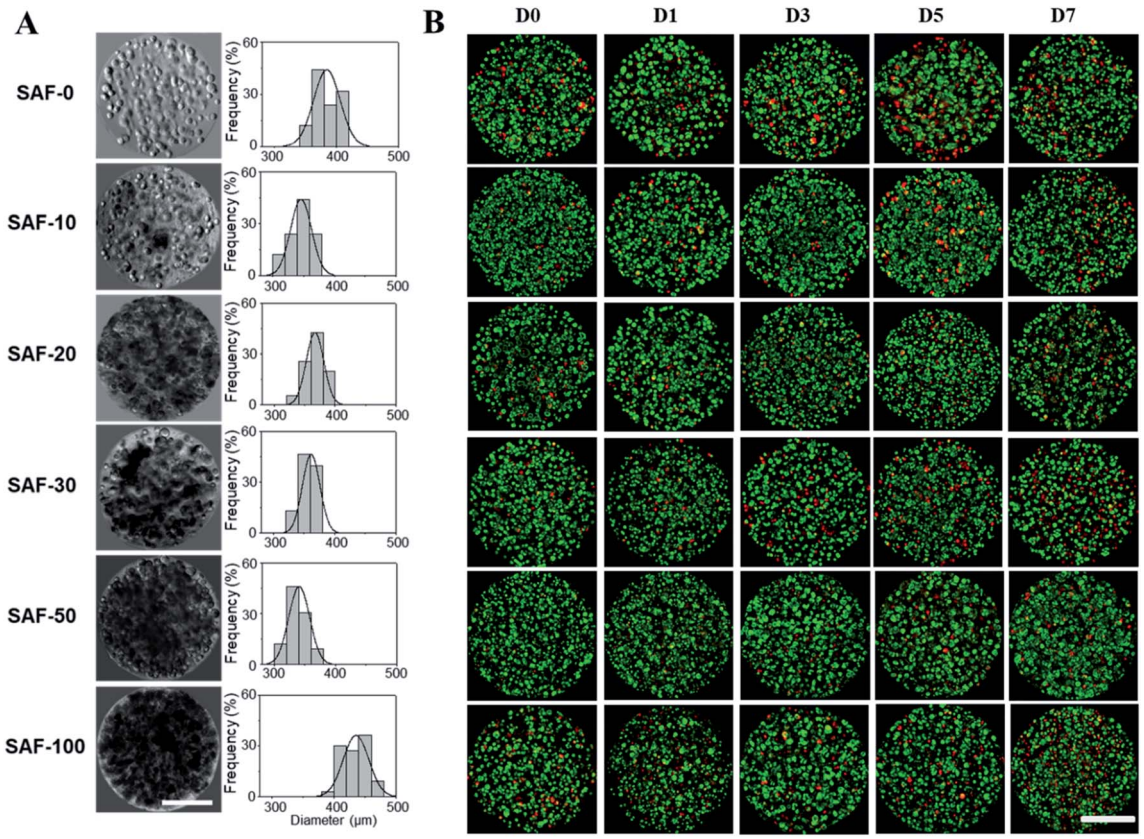

Fig. 4 Characterization of the 3D-SAF/A549 hydrogel microcapsules. (A) Optical images of representative SAF hydrogel microcapsules (left column) and their respective size distribution (right column). (B) Fluorescence images of AOPI dye stained SAF/A549 hydrogel microcapsules with different compositions (SAF-0 to SAF-100) at different time points from day 0 to 7 (D0 to D7). The green and red colors indicate live and dead cells, respectively. Cells were uniformly distributed in all compositions of the SAF microcapsules. Scale bar = 200 μm.

distributed within the microcapsules. No empty microcapsules were observed microscopically.

Size and morphology of the 3D SAF/A549 hydrogel microcapsules

In a long term and large-scale culture, keeping the shape, size, and morphology of the microcapsules intact in the culture media play an important role. From our earlier systematic investigations, the effect of processing parameters, including cell concentration, solution concentration, applied voltage, and flow rate were investigated for the production of optimal sized SAF microcapsules.[27] A substantial effect of the microcapsule composition containing both PLGA nanofibers and chitin nanofibrils on cell growth media was observed up to day 7. Among all the compositions, the SAF-100/A549 microcapsules showed a very compact density, which became denser from the outside to the inside of the microcapsules. Except for the SAF-0/A549 and SAF-100/A549 microcapsules, all of the other compositions of microcapsules showed relatively little change in size, as seen in Fig. 4A. However, with an increase in the number of culture days, a gradual increase in the microcapsule size was observed for SAF-100/A549 compared to the control SAF-0/A549 microcapsules (ESI S4†).

As a continued advancement of our earlier work on hydrogel systems,[27] the current SAF microencapsulated cells show better cell–matrix assisted cell growth. All compositions of the SAF/A549 microcapsules were cultured for up to 7 days and stained with AOPI dye, as shown in Fig. 4B, in which live and dead cells are stained in green and red, respectively. The cell image data of the microcapsules indicates that the encapsulated cells are not adversely affected by the microencapsulation process. Compared to the control, all of the SAF/A549 microcapsules are very spherical in morphology, and the cells are densely packed. However, after day 10 of culture, some of the cells had diffused out from the SAF-0 and SAF-10 microcapsules (ESI S3†).

Cell viability of the 3D SAF/A549 hydrogel microcapsules

All of the compositions of SAF/A549 microcapsules were cultured for up to 7 days. Cell viability was evaluated using the lactase dehydrogenase (LDH) assay, as shown in Fig. 5A. The dead cells per representative microcapsule were also counted using the AOPI dye staining method, as shown in Fig. 5B. Encapsulated cells in all compositions of the microcapsules were compared with the control and showed higher cell viability. The data suggest that the microencapsulation process does not adversely affect cell viability. No viability difference in the chitin nanofibrils containing the microcapsule groups up to day 3 of culture was observed. A substantial cell growth effect was noticed on day 7 in all

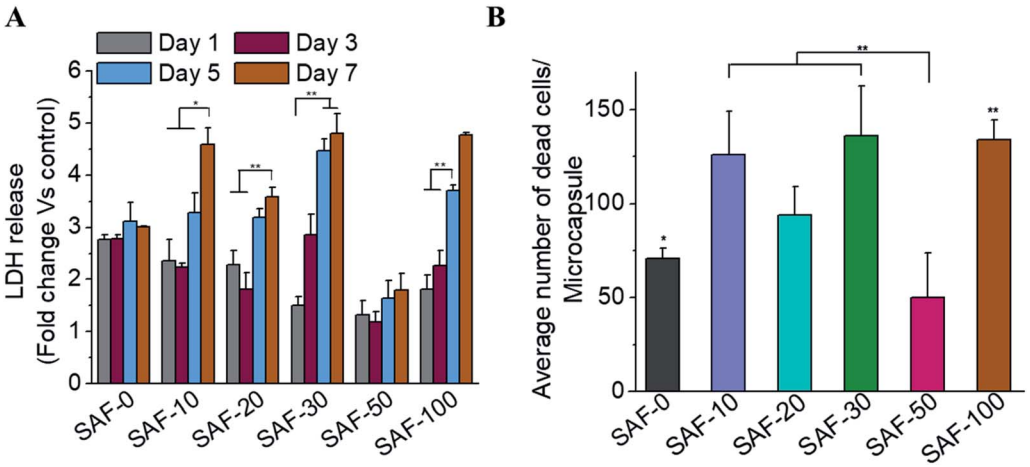

Fig. 5 Cell viability in the 3D-SAF hydrogel microcapsules. (A) Viability of the A549 cells cultured in various compositions of SAF/A549 hydrogel microcapsules for 1, 3, 5, and 7 days (LDH release assay, data were normalized to the values of the SAF-0/A549 microcapsules as a control). (B) Average number of dead cells per microcapsule measured on day 7. Data are representative of multiple experiments ($n = 3$) (ANOVA, $*p < 0.05$, $**p < 0.01$, $***p < 0.001$).

samples with chitin nanofibrils. SAF-50/A549 microcapsules show the highest rate of cell growth compared to control (SAF-0/A549) microcapsules, as shown in Fig. 5A. However, among all the tested compositions, both the LDH and AOPI staining data show that higher cell viability was observed in the SAF-50/A549 microcapsules, indicating that the optimal chitin nanofibril composition in the SAF/A549 microcapsules promotes cell proliferation, as shown in Fig. 5A. Compared to

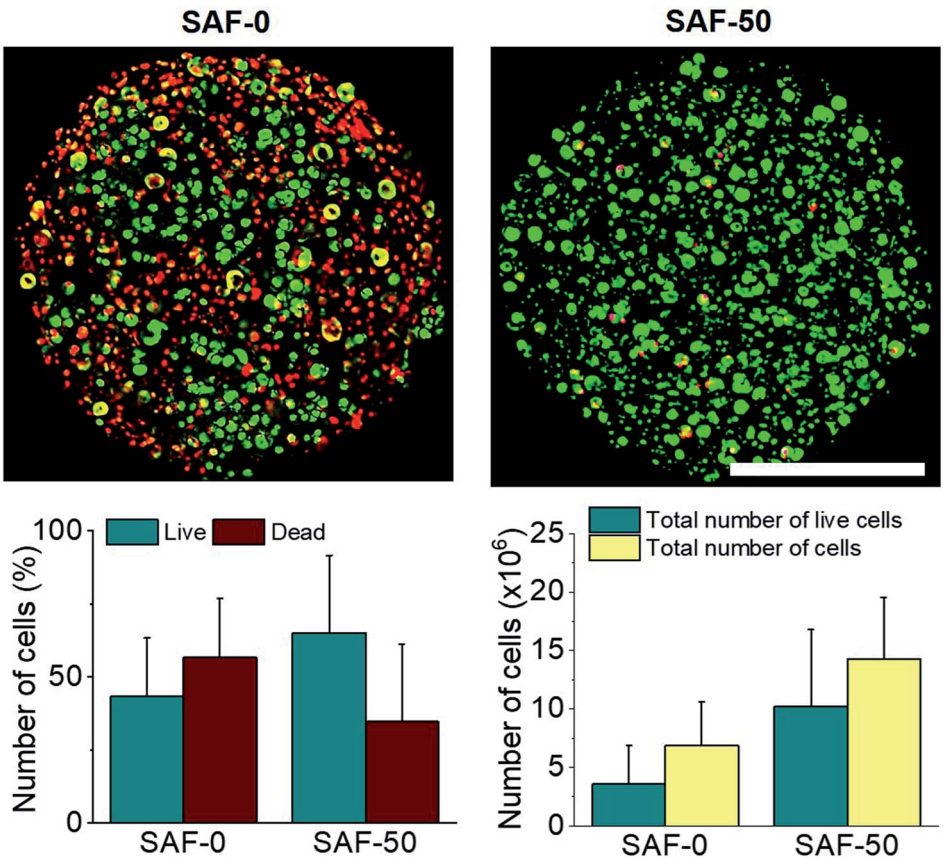

Fig. 6 Fluorescence imaging of the 3D SAF/A549 hydrogel microcapsules after long-term culture. Upper panel: fluorescent images of dye-labeled 3D SAF/A549 hydrogel microcapsules (compositions; SAF-0 and SAF-50) on day 31. The green and red colors indicate live and dead cells, respectively, and cells were uniformly distributed in the SAF microcapsules. Scale bar = 200 μm. Lower panel: the bar graph represents the counted number of live and dead cells in the representative microcapsule fluorescent images shown in the upper panel ($n = 3$).

the control, all of the microcapsules showed significantly elevated cell growth.

Long-term culture of the 3D SAF/A549 hydrogel microcapsules

Most 2D *in vitro* systems are limited to short-term cell culture due to the lack of a 3D supporting environment in which to grow and differentiate cells. Various 3D *in vitro* systems have been utilized for long-term cell culture to establish prolonged cell culture conditions that mimic *in vivo* phenotypes such as autophagic, differentiation and lipogenic character that require a continuous source of ECM-like support. On day 3, apart from the 3D SAF-50/A549 microcapsules, all the other microcapsule compositions showed high cell viability, as shown in Fig. 5A. More dead cells (red color staining) were observed from day 7 (Fig. 4B) and their number continuously increased up to day 31. Compared to the control microcapsules, cell death within the 3D SAF-50/A549 microcapsules was less pronounced up to day 31, indicating the beneficial effect of the chitin nanofibrils in the microcapsules, as shown in Fig. 6.

Nanoparticle preparation for toxicity testing with cell microcapsules

To determine the NP toxicity, a great deal of effort has been spent on the characterization of NPs. Primarily, the size, morphology, and aggregation state of NPs in aqueous test solutions has been considered. DLS and zeta potential measurements were conducted to determine the size and agglomeration of NPs, and their surface charge in aqueous media, respectively. DLS data (Fig. 7A and B) indicate that the hydrodynamic size of both types of NPs increased with their increasing concentration. The aggregate size was in the range of 30.01 ± 4.08 to 441.7 ± 22.79 nm for ZnO and 17.66 ± 1.58 to 743.9 ± 116.13 nm for Al_2O_3 under the tested media conditions at concentrations of 5 to 1000 μg mL^{-1}, respectively. The data also indicate that the aggregate size of Al_2O_3 is much larger than that of ZnO in the aqueous test media solution. The zeta potential of the NPs with increasing concentration was initially increased slightly for Al_2O_3 and continuously decreased for ZnO, as shown in Fig. 7C. However, both the size and negative zeta potential of the aggregate particles are highly unstable.

Nano-toxicity testing of the 3D SAF/A549 hydrogel microcapsules

SAF-50/A549 microcapsules were selected to assess their nanotoxicity. After culturing the microcapsules for three days, the toxicities of various concentrations of Al_2O_3, and ZnO NPs (0–250 μg mL^{-1}) were assessed. All of the NP treated microcapsules were analyzed using the Alamar Blue assay. A more pronounced sensitivity of cell toxicity was found in the ZnO rather than Al_2O_3 NPs (Fig. 7D). Comparatively, the SAF/A549 hydrogel microcapsules allow the cells to adapt an ECM mimicking microenvironment that could be closer to the *in vivo* conditions. Both types of NPs induced the dose dependent toxicity with the 3D SAF-50/A549 microcapsules.

Chemistry of 3D SAF-hydrogel microcapsules for nanoparticle assessment applications

A major component of the 3D SAF-hydrogel is a natural polyanionic linear block copolymer, sodium alginate, which contains (1–4)-linked β-D-mannuronic acid (M) and α-L-

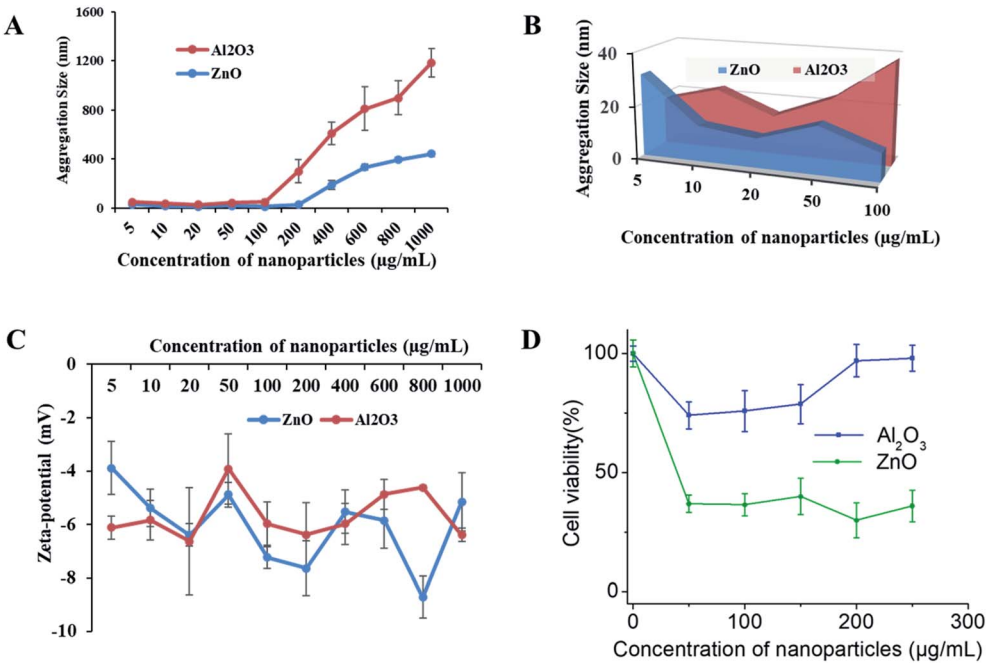

Fig. 7 Physiochemical characterization and toxicity of the NPs. Aqueous aggregation behavior and surface charge of the NPs in cell culture media solution; (A and B) hydrodynamic size of the aggregated NPs (DLS measurements), and (C) Surface charge of the NPs (zeta potential (ζ) measurements). The concentration of the NP suspension was 5 to 1000 μg mL^{-1} in complete cell-culture media. Nano-toxicity tests; (D) cell viability (Alamar Blue) after 48 h of exposure to 0–250 μg mL^{-1} of the NPs (Al_2O_3, and ZnO). The aggregate size was from 30.01 ± 4.08 to 441.7 ± 22.79 nm for ZnO and 17.66 ± 1.58 to 743.9 ± 116.13 nm for Al_2O_3 in test media with concentrations of 5 to 1000 μg mL^{-1}, respectively.

guluronic acid (G) blocks.[38] During the gelation process, cations of calcium preferably bind to the G block of the polymer chain, thereby providing rigidity to the polymer structure and leading to the formation of a stronger gel. Alginate hydrogel can have a wide range of pore size distribution (5 to 200 nm); however, it does not provide cell adhesion motifs to improve cell support.[39] In the presence of polycations such as chitin fibrils, alginates can form polyelectrolyte complexes.[40] By mimicking the exquisite architecture and functional properties of native tissues and physiological compatibility, chitin fibril-based materials have demonstrated excellent results.[41] Blending chitin fibrils with PLGA can further improve the mechanical properties and degradation time of the 3D hydrogel.[42] The degradation properties can be tuned by adjusting the amount of PLGA along with its molecular weight and the ratio of lactic acid to glycolic acid to the polymer.[43] Considering all these prerequisite properties, the 3D SAF-hydrogel microcapsules should have stable physiochemical capacity with tunable mechanical properties, and highly flexible cell adhesion motifs to house the cells for long term nanoparticle toxicity assessment (Fig. 8).

Discussion

In pharmaceutical, cellular and molecular science fields, a wide variety of 3D cell culture platforms have been developed as valuable tools for drug discovery and toxicology studies.[44] There is a pressing demand for versatile 3D cell culture platforms because the current 3D cell culture models are time-consuming, display increased variability, have less cell adhesion motifs, *etc.* Our long-term objective in this research is to develop 3D SAF-hydrogel cell constructs as a simple, rapid, cost-effective, and high-throughput 3D cell culture platform that could be later developed as a surrogate of an *in vivo* system. The production of a monodisperse SAF-hydrogel by incorporating biophysical ECM mimicking cues, including a nanonet–nanofiber network in a spherical hydrogel that mimics *in vivo*-like microenvironments has been recently developed.[27] This new nanonet–nanofiber network research has been recently published.[45] Here, we further successfully engineer the hydrogel with chitin fibrils as possible physical cell adhesion motifs. Our technique has potential for the high-throughput production of a 3D SAF-hydrogel (~800 SAF-hydrogel microcapsules per second) with uniform size and functionality.

Nanoparticle toxicity assessment is more laborious in comparison to conventional drug screening, since nanoparticles display additional physicochemical properties, such as surface area, shape, and functionality.[46] Nanoparticles can aggregate, sediment, and display different diffusion dynamics when they interact with a biological environment, particularly with the biomolecules that are present in biological fluids.[47,48] In this context, it will be challenging to identify toxic side effects that are specific only to nanoparticles. Multiple toxicity tests need to be conducted in parallel, to confirm the safety assessment results of the nanoparticles. Conventional 2D monolayer

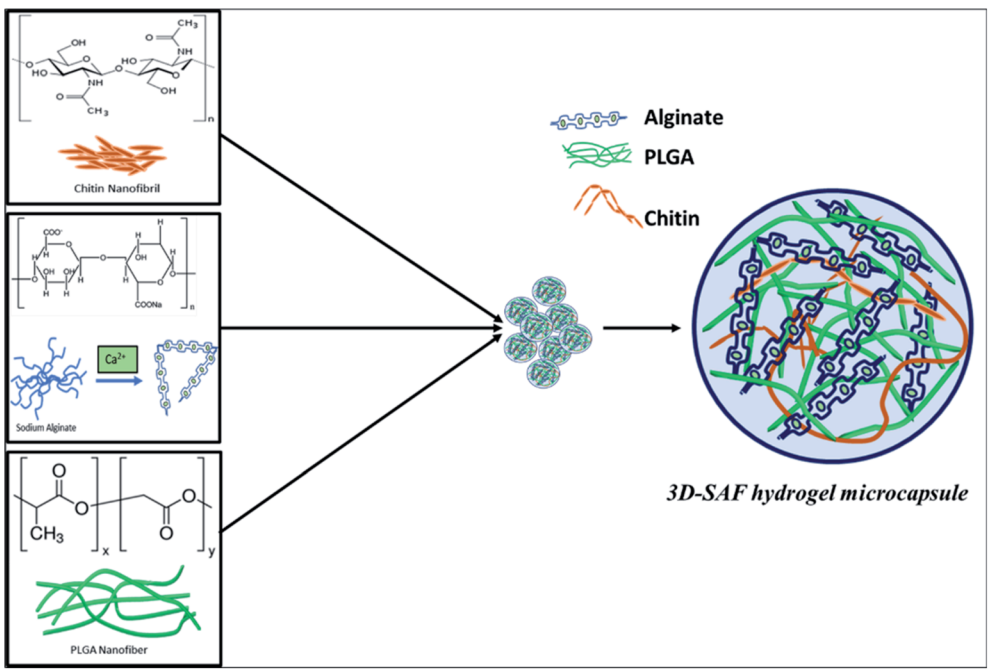

Fig. 8 Schematic diagram showing the chemical structure of the entire 3D SAF-hydrogel microcapsule. In 3D SAF-hydrogel chemistry, sodium alginate is the main material that has carboxyl groups (chelate formation) on the polymer chains, which can be cross-linked with divalent ions (Ca^{2+}). Without cations, the negatively charged carboxyl side groups repel each other, hindering the aggregation of the helices. Divalent cations can bind together two carboxyl groups producing stronger gels with an egg cage structure.[38,62] Alginates can form polyelectrolyte complexes in the presence of polycations such as chitin fibrils. Blending chitin fibrils with PLGA, a Food and Drug Administration (FDA) approved synthetic polymer, is done to obtain favorable mechanical properties and degradation time. All these mutually exclusive properties can be used to our advantage for preparing composite hydrogels with improved properties for nanoparticle toxicity assessment.

cell culture models allow the uniform distribution of colloidal nanoparticles in only one direction (on the top of monolayer cells) that does not mimic the cell architecture like under *in vivo* conditions. Dynamic and realistic models, like 3D microcapsule can be used to predict more realistic interactions of nanoparticles with cells in multiple directions that thereby affect intracellular toxicity kinetics. In this regard, the design of safe and effective 3D SAF-hydrogel cellular constructs that mimic various aspects of solid tissue cells (surface-exposed and deeply buried cells, and proliferating and non-proliferating cells) can facilitate safety assessment tests that could give predictive information about nanoparticle activity. Additionally, precisely cultured single 3D SAF-hydrogel cellular constructs in high throughput with a specialized plate reader platform provide rapid, precise, and reproducible results with the minimum use of reagents and biological samples. 3D SAF-hydrogel microcapsules should have stable physiochemical capacity, tunable mechanical properties, and flexible cell adhesion motifs for nanoparticle assessment application.

Herein, we report a novel strategy to design 3D-SAF hydrogel microcapsules using one-step A549 cell encapsulation. These microcapsules can be developed as a potential 3D toxicity testing device for general application as a short term goal, and as a pharmaceutical drugs toxicity screening device as a long-term goal.[14,18,26,49] This investigation is a further expanded approach of our previously reported PNA hydrogel microcapsules.[27]

The first objective of this study was to construct a fibrous hydrogel microcapsule with random layers of both synthetic and natural nanofibers/nanofibrils for the purpose of developing a better microenvironment for cell growth and proliferation. The impact of PLGA nanofibers on SAF microcapsules was previously optimized[27] and suggested that 10% of fibers in microcapsules improved the overall suitability for cell growth compared to microcapsules without fibers. The poor mechanical properties of the alginate hydrogel correlate with its poor capability of maintaining a desired 3D shaped architecture for long term applications. Incorporation of PLGA nanofibers in the microsphere help to maintain the 3D framework of the alginate hydrogel in the short term. However, PLGA alone has some limitations, such as low cell affinity due to hydrophobicity and lack of cell recognition sites. The combination of both synthetic and natural fibers can be used to design microcapsules with enhanced biodegradability, cell attachment and hydrophilicity. Chitin is one of the widely used natural polymers as it has natural ability to promote cell adhesion without additional functionalization. The right blending of two types of nanofibers originated from both natural and synthetic polymers has been demonstrated to promote the higher water uptake and balanced mechanical behavior, degradability, and biological performance of the 3D cell culture system. Here, we further optimized the SAF-l0 microcapsule performance of our earlier findings with an increasing amount of chitin nanofibrils in the microcapsules. These results provide baseline information to improve the design and configuration of the material for optimal *in vitro* cell growth and development. Based on previously published results, the 3D-SAF microcapsules were expected to have a superior 3D architecture compared to the control alginate hydrogel microcapsules due to the ECM mimicking features of the nanofibers/nanofibrils along with their other properties such as softness, super-absorbency, biodegradability, and biocompatibility.

Long-term mechanical stability is considered to be a major concern in the design of microcapsules for cell immobilization, where the stability of microcapsules needs to prolong *in vivo* functions. The incorporation of both mechanical and biological signals into a single 3D-SAF microcapsule construct serves as an ECM architecture for cell replication through cellular and anatomical pathways. All of the tested physical and mechanical results support our hypothesis that the PLGA nanofibers/chitin nanofibril-containing microcapsules closely replicate natural ECM features.

The second objective of this study was to encapsulate A549 cells by adapting the previously published encapsulation conditions and the production of smooth microcapsules with an average diameter of around or below 500 μm.[27] The production of highly controlled monodisperse 3D SAF/A549 microcapsules is needed to meet the requirement of different cells storage environment. Uniform cell-encapsulates offer more reliable outcomes since the encapsulated cells respond differently in terms of diffusion, and the transport of oxygen and nutrients varies according to the microcapsule size. Our mechanical test data indicates an increase in the stiffness of the material as the amount of chitin increases. SAF-100 shows the highest Young's modulus (YM), which is an indication of it high rigidity within microsphere environment with less porosity. There is always a need to balance porosity and mechanical strength to achieve maximum cell proliferation. Nevertheless, the YM of SAF-20 to SAF-50 are comparable, and their cell viability data indicate that more cells die in all compositions, except for in SAF-50. Our assumptions are that the amount of chitin in SAF-50 is optimal in promoting the porosity and diffusion of the sample and helps to transport sufficient nutrients to the cells. The amount of chitin in SF-50 is adequate for the absorption and transport of cell reagents throughout the microsphere, while the other compositions (SAF-0 to SAF-30) were inadequate. However, again SAF-100 has the highest chitin composition, but because of its densely packed environment due to strong ionic crosslinking between the alginate and chitin, cells were unable to proliferate fully compared to in SAF-50.

The viability of A549 cells 24 h post-encapsulation was more than 97% compared to the control. This indicates that the 3D SAF/A549 microcapsules have improved overall suitability for cell proliferation, toxicity, and metabolic activity compared to the control microcapsules.

The third objective of this study was to use 3D SAF/A549 microcapsules as a toxicity testing platform to study NP toxicity. The toxicity of NPs strongly depends on their size and shape, and other factors such as chemical composition and physicochemical stability of NPs in the testing media.[50] First, we determined the effect of the exposure solution in complete cell culture media (DMEM with 10% FBS) on the stability of the NPs (Al_2O_3, and ZnO). The mean hydrodynamic diameter and zeta potential of the NPs in the exposure solution were measured. The original diameter of the Al_2O_3 and ZnO particles was approximately 30 nm, however, when the NPs were suspended

in the exposure solution at various concentrations, the particle size increased rapidly and reached 1700–1900 nm. The agglomerate sizes of the NPs were beyond their original nanoscale size in the exposure solution, but they were still different from their bulk counterparts.[51] No significant changes in zeta potential were observed at different concentrations of NPs. The zeta potential of the NPs was approximately 20 mV in solution. It has been reported that when the zeta potential is between 30 and 20 mV, the NP suspension is unlikely to be stable and is prone to aggregation. Next, 3D SAF-50/A549 microcapsules were treated with increasing concentrations of NPs. More pronounced sensitivity of cell toxicity was observed for ZnO compared to the Al_2O_3 NPs at different concentrations (1–100 μg mL^{-1}).[52] The cytotoxicity of the NPs was much lower compared to a published monocultured cell type than that observed in the 3D spheroids.[53,54] Thus, as suggested, 2D systems may overestimate chemical toxicity, ascribable to the absence of 3D organization, and confer some mechanical resistance to cytoskeletal disruption.

Taking all the data together, the 3D SAF-50/A549 microcapsules exhibit many ECM-like features that are closer to complex *in vivo* conditions. Our findings suggest that the PLGA nanofiber/chitin nanofibril incorporated microcapsules improve the overall suitability for cell proliferation, toxicity, and metabolic activity compared to microcapsules without PLGA nanofibers as a control.[27] Significant attenuation of NP-induced toxicity was detected in 3D microcapsules compared to that obtained in the respective monocultures. Importantly, one of the great advantages of using 3D SAF-50/A549 microcapsule models is the possibility of repeat-dosing, as we confirmed their viability and functionality over a long period (*i.e.*, 30 days), compared to 2D TCP monolayer cultures.

Our ongoing work is particularly focused on the further development of 3D SAF-hydrogel microcapsules for high-throughput screening platforms. The culture of a single 3D SAF-hydrogel in a micro-well significantly reduces the cell culture reagents required due to the minute volume needed to grow the cells, which significantly reduces the dose and volume of testing materials, especially NPs. A major bottleneck in NP screening applications is the screening of the response of 3D hydrogel cell constructs with NPs in a high-throughput manner followed by the quick analysis of a large amount of screening data. However, the 3D SAF-hydrogel cell construct can be readily analyzed through imaging and biochemical assay techniques. Analysis of the supernatants of culture media with a specialized plate reader and direct imaging (*e.g.*, using light, fluorescence, and confocal microscopy) of the 3D SAF-hydrogel microcapsules in a well or Transwell microplate without further processing of the 3D cells provide excellent opportunity for high-throughput screening (HTS) of toxicants and drugs *via* rapid and precise analysis.

Our ongoing work on this system is focused on the further development of high throughput application devices not only for toxicity screening but also for clinical assays and disease diagnosis using a specialized plate reader and automatic dispenser tool. The precise dispensing of single 3D SAF-hydrogel microcapsules per well in a microplate using an automatic robotic tool is quite challenging, and there is still room for the optimization of this process. However, with our manual repeater dispensing system using wide bore filtered pipette tips, we can transfer single SAF-hydrogel microcapsules into the wells of a microplate. Pipette tip selection is also another critical factor to prevent further damage of microcapsules during the transfer process. Special pipette tips with a super slippery surface can help to reduce the shear force imposed and improve the retention of the sample.

Conclusions

In summary, we designed and characterized different compositions of 3D SAF microcapsules *via* electrostatic encapsulation of cryofractured PLGA nanofibers, chitin fibrils and alginate hydrogel. Our findings suggest that the 3D SAF-50 microcapsules show improved overall suitability for cell proliferation, toxicity, and metabolic activity compared to 3D SAF-0 microcapsules as a control. 3D SAF-50 microcapsules overcome the limitation of alginate hydrogels as its properties can be controlled compared with other hydrogel compositions. Fibrous hydrogels of 3D SAF-50 with an interpenetrating network structure formed from alginate and nanofibrils/nanofibers show controllable mechanical properties, and provide cell adhesion support, thus facilitating cell growth. Therefore, the present method of 3D SAF-50 hydrogel microcapsule preparation provides a simple and straightforward approach to enhance the mechanical strength of the microcapsules compared to our previously reported approaches.[27] The newly designed 3D SAF-50 hydrogel microcapsules emerge as a promising 3D *in vitro* model with ECM mimicking features and can be utilized to build high throughput toxicity screening platforms to study NP toxicity. This study also paves the way to develop patient-derived organoids, which can serve as a bridge toward *in vivo* animal models to replace human pre-clinical trials.

Materials and methods

Materials

Commercial NPs of ZnO and Al_2O_3 were obtained from Nanostructured & Amorphous Materials, Inc., Katy, TX, USA. The mean diameter of the Al_2O_3 particles (CAS# 1344-28-1) was 30 ± 10 nm, and the crystalline phase of the Al_2O_3 particle was gamma. The mean diameter of the ZnO particles (Stock # 5811HT) and their specific surface areas were 30 nm and 15 m^2 g^{-1}, respectively. Poly(lactic-*co*-glycolic acid) (PLGA, 75 : 25; Durect Corporation (Birmingham, AL, USA)), chitin (Millipore Sigma, St. Louis, MO, USA), and alginate (Novamatrix, Industriveien 33 N-1337 Sandvika Norway), Dulbecco's Modified Eagle's Medium (DMEM) supplemented with 10% fetal bovine serum (FBS) (Invitrogen, Waltham, MA, USA), 1% pen strip (100×) (Life Technology, Gaithersburg, MD, USA) and 0.12% insulin (Life Technology, Gaithersburg, MD, USA) were the major materials used in this project.

Production of cryoground PLGA nanofibers

PLGA (75 : 25, inherent viscosity 0.55–0.75 dL g^{-1}), was purchased from Durect Corporation (Birmingham, AL, USA).

The electrospun nanofiber mesh of PLGA was prepared as described in previous publications using PLGA solutions in a mixture of chloroform and DMF (80 : 20) and a custom built electrospinning instrument.[55–58] Cryoground PLGA nanofibers were obtained using a cryogrinding process as described previously.[27,59,60]

Chitin nanofibril fabrication

Chitin (from shrimp shells, BioReagent) was purchased from Sigma Aldrich (Millipore Sigma, St. Louis, MO, USA). Chitin nanofibrils were fabricated using a nano-fibrillation process.[61] In brief, 4% (w/v) chitin powder was mixed in deionized (DI) water. The mixed solution was subjected to probe ultrasonic treatments under N_2 gas bubbling at ice-cold temperatures for 3 h. The resulting chitin nanofibril suspension was sterilized under UV light before mixing it with alginate solution.

Production of SAF hydrogel microcapsules

The fabrication of SAF microcapsules was achieved *via* the integration of electrospinning and electrospraying techniques as described in our previous publications.[27] Briefly, 2% (w/v) ultra-pure alginate (PRONOVA UP MVG, Novamatrix, Industriveien 33 N-1337 Sandvika Norway) was dissolved in 1× HBSS buffer (Life Technology, Gaithersburg, MD, USA). Cryoground PLGA nanofibers and chitin nanofibrils were mixed in different weight percentages of the dry weight of alginate. See details of the SAF microcapsule composition in ESI Table T1† (*i.e.*, SAF-0 to SAF-100). For better dispersion, the PLGA nanofibers and chitin nanofibrils were dispersed in DI water under sonication and then mixed with alginate solution. The mixed solution was drawn into a syringe fitted with a 24-gauge needle and then loaded onto a syringe pump for electrospraying using the pre-defined setup conditions as reported in a previous publication.[27] The microcapsules without cryoground PLGA nanofibers and chitin nanofibrils were used as control microcapsules (denoted as SAF-0).

Morphology and stability of the SAF hydrogel microcapsules

The morphology of the fabricated SAF microcapsules was studied using an optical microscope (EVOS® XL Core Imaging System) under cell culture conditions. The size distributions of the microcapsules were measured from optical images using ImageJ software. The stability of the SAF microcapsules was studied by incubating them in 24 well plates with complete DMEM culture media for 15 days.

Mechanical properties of the SAF hydrogel microcapsules

The mechanical properties of the as-prepared microcapsules were measured using a two parallel plate compressive system (MicroTester—Cell Scale Biomaterials Testing, Waterloo, Canada). Microcapsules ($n = 3$ for each composition) were placed on a fixed flat stage, maintained at 37 °C in DI water, and a constant force was applied through a circular tungsten microbeam with a length and diameter of 58 and 0.5588 mm, respectively. Spheres were compressed to a maximum of 30% of their original diameter for 20 seconds and force–displacement curves were recorded according to the software provided by the company (MicroTester G2).

A549 cell culture

A549 cells (human epithelial cell line derived from a lung carcinoma tissue, ATCC® CCL-185™), were maintained in standard DMEM supplemented with 10% FBS (Invitrogen, Waltham, MA, USA), 1% pen strip (100×) (Life Technology, Gaithersburg, MD, USA) and 0.12% insulin (Life Technology, Gaithersburg, MD, USA). The cells were grown in 75 cm^2 tissue culture flasks at 37 °C in a 5% CO_2 humidified environment. At 80% confluence, cells were trypsinized with 0.25% trypsin/EDTA (Invitrogen, Waltham, MA, USA), pelleted by centrifugation, and finally resuspended with fresh medium to the desired cell density.

Cell encapsulation in the SAF hydrogel microcapsules (3D SAF/A549)

The encapsulation method was adapted from a previous publication.[27] Briefly, A549 cells at a density of 1.5×10^7 cells per mL were suspended in alginate solution (with or without SAF) in a 1 : 1 ratio, and electrosprayed under the same conditions as described in the SAF microcapsules section. 3D SAF/A549 was cultured under the same conditions as described for the A549 cells. The culture media was changed and replenished with fresh warm (37 °C) complete DMEM medium at each time point per experimental setting. The changed media were collected and stored at −20 °C for further analysis. The morphology and size distribution were also analyzed as described in the method in the previous section.

Alamar Blue assay

The cell viability was monitored using the Alamar Blue assay according to the manufacturer's standard protocol as described in an earlier publication.[27] Briefly, at a specific time point, the cell culture medium was collected from each of the 3D SAF/A549 incubated samples and stored for toxicity study. Then, the 3D SAF/A549 was washed twice with PBS and incubated for 4 h with 10% (v/v) AB reagent in the respective culture medium. Assay solutions were transferred to fresh well plates to measure their fluorescence excitation at 530 nm and emission at 590 nm. Cell viability was calculated using the following equation:

$$\text{Cell viability} = (\text{fluorescence of the samples} - \text{the fluorescence of the blank})/(\text{the fluorescence of the control} - \text{the fluorescence of the blank}) \times 100\%$$

Fluorescence imaging and analysis

Fluorescence imaging of 3D SAF/A549 was performed by staining with AOPI dye (Nexcelom Bioscience, Lawrence, MA) as previously reported.[27] Briefly, at different time points, cultured media was aspirated from the wells, and the microcapsules were washed with DPBS twice to remove FBS. They were then stained

with 15 μL of dye and incubated at 37 °C for 10 min. Z-stack fluorescence images were photographed under an Olympus IX83 microscope using Olympus cell Sens Dimension software (Olympus Corporation, Shinjuku, Tokyo, Japan).

LDH assay

LDH was quantified in the collected media at different time periods using a Pierce LDH cytotoxicity assay kit (Thermo Scientific, Catalog # 88953, Waltham, MA, USA) as previously reported.[27] Briefly, 50 μL of each collected sample medium was transferred to a 96-well flat-bottom plate in triplicate wells along with the LDH positive control (as mentioned in the kit) and blank media as a negative control. Then, 50 μL of the reaction mixture was added to each well, and the plate was incubated at room temperature for 30 minutes in the dark. The reaction was stopped by adding 50 μL of Stop Solution to each of the sample wells and mixing *via* gentle tapping. The absorbance of the assay solution was measured on a microplate reader (BioTek Inc., Winooski, VT, USA) at wavelengths of 490 and 680 nm to calculate the cytotoxicity.

De-gelation of the 3D SAF/A549 microcapsules for live and dead cell counts

The 3D SAF/A549 microcapsules were subjected to a de-gelation process to count the live and dead cells. In brief, microcapsules of 3D SAF/A549 were collected and transferred to vials. 1–1.5 mL of 100 mM sodium citrate solution was added to each vial, which were then gently shaken for 90 seconds. Cells were then pelleted by centrifugation at 4000 rpm for 3 minutes. The supernatant was discarded, and cells were resuspended with fresh medium and counted using a Countess™ II Automated Cell Counter (Thermo Fisher Scientific).

Nanoparticle solution preparation and toxicity testing

ZnO and Al_2O_3 particles were suspended in DI water (5 to 1000 μg mL^{-1}) under sonication in a water bath for 30 min (representative TEM images are provided in S5 in the ESI S5†). DMEM containing 10% FBS was then added to the NP solution and mixed vigorously *via* vortexing to create the exposure solution. The hydrodynamic size and zeta potential of the NPs were monitored using a Zetasizer Nano ZS (Malvern, Worcestershire, UK) at concentrations of 5 to 1000 μg mL^{-1}. The analysis was repeated three times, and the average of all of the values was calculated. For the toxicity testing, the prepared NP solution was transferred into the 24 well plates containing 3D SAF/A549 (the number of SAF hydrogel microcapsules per well was kept constant; at approximately 100); and then NP exposed 3D SAF/A549 was cultured under the same conditions as described for the A549 cells. The culture media was changed and replenished with fresh warm (37 °C) complete DMEM media at each of the time points per experimental setting. The changed media was collected and stored at −20 °C for further LDH analysis in 96 well plates, and the morphology and size distribution of 3D SAF/A549 were also analyzed as described in previously published methods.

Statistical analysis

All results were expressed as mean ± S.D. Data were analyzed for significance with OriginPro software (Origin Lab, Northampton, MA, USA) using one-way analysis of variance (ANOVA). A post hoc Tukey's test was performed with ANOVA for multiple comparisons. The α-value was set to 0.05 and p-values of less than 0.05 were considered statistically significant.

Conflicts of interest

There are no conflicts to declare.

Acknowledgements

This work was supported financially by the National Science Foundation, through the Engineering Research Center for Revolutionizing Metallic Biomaterials (ERC-RMB, EEC-0812348). Characterization of the microcapsules was also performed in part at the Joint School of Nanoscience and Nanoengineering, a member of the Southeastern Nanotechnology Infrastructure Corridor (SENIC) and the National Nanotechnology Coordinated Infrastructure (NNCI), which is supported by the National Science Foundation (NSF ECCS-1542174).

References

1 J. Cheon, W. Chan and I. Zuhorn, The Future of Nanotechnology: Cross-disciplined Progress to Improve Health and Medicine, *Acc. Chem. Res.*, 2019, **52**, 2405.
2 E. J. Hackett and Society for Social Studies of Science, *The handbook of science and technology studies*, MIT Press, Published in cooperation with the Society for the Social Studies of Science, Cambridge, Mass, 3rd edn, 2008.
3 A. Moore, Brave small world. Biotechnology and nanotechnology may give rise to a completely new industry, *EMBO Rep.*, 2001, **2**, 86–88.
4 A. M. Holmes, L. Mackenzie and M. S. Roberts, Disposition and measured toxicity of zinc oxide nanoparticles and zinc ions against keratinocytes in cell culture and viable human epidermis, *Nanotoxicology*, 2020, **14**, 263–274.
5 C. Teng, J. Jia, Z. Wang and B. Yan, Oral Co-Exposures to zinc oxide nanoparticles and $CdCl_2$ induced maternal-fetal pollutant transfer and embryotoxicity by damaging placental barriers, *Ecotoxicol. Environ. Saf.*, 2020, **189**, 109956.
6 G. R. Tortella, *et al.*, Silver nanoparticles: toxicity in model organisms as an overview of its hazard for human health and the environment, *J. Hazard. Mater.*, 2020, **390**, 121974.
7 L. Mu and R. L. Sprando, Application of nanotechnology in cosmetics, *Pharm. Res.*, 2010, **27**, 1746–1749.
8 J. H. Zippin and A. Friedman, Nanotechnology in cosmetics and sunscreens: an update, *J. Drugs Dermatol.*, 2009, **8**, 955–958.
9 J. Park, in *Concise Encyclopedia of Advanced Ceramic Materials*, Elsevier, 1991, pp. 13–16.

10 J. B. Park, in *Concise Encyclopedia of Advanced Ceramic Materials*, ed. R. J. Brook, Pergamon, Oxford, 1991, pp. 13–16.
11 N. A. Kotov, Politics and nanotechnology in the health care industry, *ACS Nano*, 2009, **3**, 2855–2856.
12 J. Jia, *et al.*, Crossing Biological Barriers by Engineered Nanoparticles, *Chem. Res. Toxicol.*, 2020, **33**, 1055–1060.
13 G. R. Jackson Jr, A. G. Maione, M. Klausner and P. J. Hayden, Prevalidation of an Acute Inhalation Toxicity Test Using the EpiAirway *In Vitro* Human Airway Model, *Appl. In Vitro Toxicol.*, 2018, **4**, 149–158.
14 S. Y. Shaw, *et al.*, Perturbational profiling of nanomaterial biologic activity, *Proc. Natl. Acad. Sci. U. S. A.*, 2008, **105**, 7387–7392.
15 T. Limongi, *et al.*, Improving dispersal of therapeutic nanoparticles in the human body, *Nanomedicine*, 2019, **14**, 797–801.
16 J. Lee, *et al.*, Safety assessment of cerium oxide nanoparticles: combined repeated-dose toxicity with reproductive/developmental toxicity screening and biodistribution in rats, *Nanotoxicology*, 2020, 1–15.
17 R. Pecoraro, *et al.*, Metallic Nano-Composite Toxicity Evaluation by Zebrafish Embryo Toxicity Test with Identification of Specific Exposure Biomarkers, *Curr. Protoc. Toxicol.*, 2017, **74**, 1.14.11–11.14.13.
18 E. Frohlich, Comparison of conventional and advanced *in vitro* models in the toxicity testing of nanoparticles, *Artif. Cells, Nanomed., Biotechnol.*, 2018, **46**, 1091–1107.
19 M. Siegrist, A. Wiek, A. Helland and H. Kastenholz, Risks and nanotechnology: the public is more concerned than experts and industry, *Nat. Nanotechnol.*, 2007, **2**, 67.
20 V. Murashov, P. Schulte, C. Geraci and J. Howard, Regulatory approaches to worker protection in nanotechnology industry in the USA and European union, *Ind. Health*, 2011, **49**, 280–296.
21 J. Lojk, J. Repas, P. Veranic, V. B. Bregar and M. Pavlin, Toxicity mechanisms of selected engineered nanoparticles on human neural cells *in vitro*, *Toxicology*, 2020, **432**, 152364.
22 M. M. Sufian, J. Z. K. Khattak, S. Yousaf and M. S. Rana, Safety issues associated with the use of nanoparticles in human body, *Photodiagn. Photodyn. Ther.*, 2017, **19**, 67–72.
23 D. A. van Dartel and A. H. Piersma, The embryonic stem cell test combined with toxicogenomics as an alternative testing model for the assessment of developmental toxicity, *Reprod. Toxicol.*, 2011, **32**, 235–244.
24 K. Duval, *et al.*, Modeling Physiological Events in 2D *vs.* 3D Cell Culture, *Physiology*, 2017, **32**, 266–277.
25 F. Pampaloni, E. G. Reynaud and E. H. Stelzer, The third dimension bridges the gap between cell culture and live tissue, *Nat. Rev. Mol. Cell Biol.*, 2007, **8**, 839–845.
26 F. Saleh, A. Harb, N. Soudani and H. Zaraket, A three-dimensional A549 cell culture model to study respiratory syncytial virus infections, *J. Infect. Public Health.*, 2020, **13**(8), 1142–1147.
27 S. Khanal, *et al.*, Nano-fibre Integrated Microcapsules: A Nano-in-Micro Platform for 3D Cell Culture, *Sci. Rep.*, 2019, **9**, 13951.
28 S. A. Langhans, Three-dimensional *in vitro* cell culture models in drug discovery and drug repositioning, *Front. Pharmacol.*, 2018, **9**, 6.
29 S. A. Langhans, Three-Dimensional *in Vitro* Cell Culture Models in Drug Discovery and Drug Repositioning, *Front. Pharmacol.*, 2018, **9**, 6.
30 X. Zhang, *et al.*, Three-Dimensional Printed Cell Culture Model Based on Spherical Colloidal Lignin Particles and Cellulose Nanofibril-Alginate Hydrogel, *Biomacromolecules*, 2020, **21**, 1875–1885.
31 S. R. Caliari and J. A. Burdick, A practical guide to hydrogels for cell culture, *Nat. Methods*, 2016, **13**, 405–414.
32 B. M. Baker and C. S. Chen, Deconstructing the third dimension: how 3D culture microenvironments alter cellular cues, *J. Cell Sci.*, 2012, **125**, 3015–3024.
33 J. E. Samorezov, C. M. Morlock and E. Alsberg, Dual Ionic and Photo-Crosslinked Alginate Hydrogels for Micropatterned Spatial Control of Material Properties and Cell Behavior, *Bioconjugate Chem.*, 2015, **26**, 1339–1347.
34 T. Andersen, P. Auk-Emblem and M. Dornish, 3D Cell Culture in Alginate Hydrogels, *Microarrays*, 2015, **4**, 133–161.
35 S. Nam, R. Stowers, J. Lou, Y. Xia and O. Chaudhuri, Varying PEG density to control stress relaxation in alginate–PEG hydrogels for 3D cell culture studies, *Biomaterials*, 2019, **200**, 15–24.
36 X. Su, *et al.*, Hierarchical microspheres with macropores fabricated from chitin as 3D cell culture, *J. Mater. Chem. B*, 2019, **7**, 5190–5198.
37 C. Moser, *et al.*, A Perfusion Culture System for Assessing Bone Marrow Stromal Cell Differentiation on PLGA Scaffolds for Bone Repair, *Front. Bioeng. Biotechnol.*, 2018, **6**, 161.
38 M. Szekalska, A. Puciłowska, E. Szymańska, P. Ciosek and K. Winnicka, Alginate: Current Use and Future Perspectives in Pharmaceutical and Biomedical Applications, *Int. J. Polym. Sci.*, 2016, 7697031.
39 L. Gasperini, J. F. Mano and R. L. Reis, Natural polymers for the microencapsulation of cells, *J. R. Soc., Interface*, 2014, **11**, 20140817.
40 V. A. Petrova, *et al.*, Alginate Gel Reinforcement with Chitin Nanowhiskers Modulates Rheological Properties and Drug Release Profile, *Biomolecules*, 2019, **9**, 291.
41 K. Sato, K. Tanaka, Y. Takata, K. Yamamoto and J.-I. Kadokawa, Fabrication of cationic chitin nanofiber/alginate composite materials, *Int. J. Biol. Macromol.*, 2016, **91**, 724–729.
42 F. L. Mi, *et al.*, Chitin/PLGA blend microspheres as a biodegradable drug delivery system: a new delivery system for protein, *Biomaterials*, 2003, **24**, 5023–5036.
43 H. K. Makadia and S. J. Siegel, Poly Lactic-*co*-Glycolic Acid (PLGA) as Biodegradable Controlled Drug Delivery Carrier, *Polymers*, 2011, **3**, 1377–1397.
44 R. Edmondson, J. J. Broglie, A. F. Adcock and L. Yang, Three-dimensional cell culture systems and their applications in drug discovery and cell-based biosensors, *Assay Drug Dev. Technol.*, 2014, **12**, 207–218.

45 S. Saudi, *et al.*, Nanonet-nano fiber electrospun mesh of PCL–chitosan for controlled and extended release of diclofenac sodium, *Nanoscale*, 2020, **12**(46), 23556–23569.
46 M. E. Davis, Z. G. Chen and D. M. Shin, Nanoparticle therapeutics: an emerging treatment modality for cancer, *Nat. Rev. Drug Discovery*, 2008, **7**, 771–782.
47 Y. Yang, *et al.*, Toxicity assessment of nanoparticles in various systems and organs, *Nanotechnol. Rev.*, 2017, **6**, 279–289.
48 D. T. Savage, J. Z. Hilt and T. D. Dziubla, *In Vitro* Methods for Assessing Nanoparticle Toxicity, *Methods Mol. Biol.*, 1894, 1–29.
49 Q. Wu, *et al.*, Bionic 3D spheroids biosensor chips for high-throughput and dynamic drug screening, *Biomed. Microdevices*, 2018, **20**, 82.
50 J. Lee, G. D. Lilly, R. C. Doty, P. Podsiadlo and N. A. Kotov, *In vitro* toxicity testing of nanoparticles in 3D cell culture, *Small*, 2009, **5**, 1213–1221.
51 L. Voss, *et al.*, Environmental Impact of ZnO Nanoparticles Evaluated by *in Vitro* Simulated Digestion, *ACS Appl. Nano Mater.*, 2020, **3**, 724–733.
52 R. Shrivastava, S. Raza, A. Yadav, P. Kushwaha and S. J. Flora, Effects of sub-acute exposure to TiO_2, ZnO and Al_2O_3 nanoparticles on oxidative stress and histological changes in mouse liver and brain, *Drug Chem. Toxicol.*, 2014, **37**, 336–347.
53 S. Dobretsov, *et al.*, Toxicity of different zinc oxide nanomaterials at three trophic levels: implications for development of low-toxicity antifouling agents, *Environ. Toxicol. Chem.*, 2020, 1343–1354.
54 A. Czyzowska and A. Barbasz, Effect of ZnO, TiO_2, Al_2O_3 and ZrO_2 nanoparticles on wheat callus cells, *Acta Biochim. Pol.*, 2019, **66**, 365–370.
55 N. P. Rijal, *et al.*, Magnesium oxide-poly(ε-caprolactone)-chitosan-based composite nanofiber for tissue engineering applications, *J. Mater. Sci. Eng. B*, 2018, **228**, 18–27.
56 M. A. Boakye, N. P. Rijal, U. Adhikari and N. Bhattarai, Fabrication and characterization of electrospun PCL–MgO–keratin-based composite nanofibers for biomedical applications, *Materials*, 2015, **8**, 4080–4095.
57 N. P. Rijal, *et al.*, Magnesium oxide-poly(ε-caprolactone)-chitosan-based composite nanofiber for tissue engineering applications, *J. Mater. Sci. Eng. B*, 2018, **228**, 18–27.
58 M. A. D. Boakye, N. P. Rijal, U. Adhikari and N. Bhattarai, Fabrication and Characterization of Electrospun PCL–MgO–Keratin-Based Composite Nanofibers for Biomedical Applications, *Materials*, 2015, **8**, 4080–4095.
59 P. Knotek, *et al.*, Cryogenic grinding of electrospun poly-ε-caprolactone mesh submerged in liquid media, *Mater. Sci. Eng., C*, 2012, **32**, 1366–1374.
60 P. Knotek, *et al.*, Cryogenic grinding of electrospun poly-ε-caprolactone mesh submerged in liquid media, *Mater. Sci. Eng. C*, 2012, **32**, 1366–1374.
61 K. Tanaka, K. Yamamoto and J.-i. Kadokawa, Facile nanofibrillation of chitin derivatives by gas bubbling and ultrasonic treatments in water, *Carbohydr. Res.*, 2014, **398**, 25–30.
62 T. E. Jørgensen, Influence of oligoguluronates on alginate gelation, kinetics, and polymer organization, *Biomacromolecules*, 2007, **8**(8), 2388–2397.